available at www.sciencedirect.com

ScienceDirect

www.elsevier.com/locate/brainres

BRAIN RESEARCH

Research Report

Nesfatin-1 inhibits NPY neurons in the arcuate nucleus

Christopher J. Price[a], *Willis K. Samson*[b], *Alastair V. Ferguson*[a,*]

[a]*Department of Physiology, Queen's University, Kingston, ON, Canada, K7L 3N6*
[b]*Pharmacological and Physiological Science, St. Louis University School of Medicine, St. Louis, USA*

ARTICLE INFO

Article history:
Accepted 24 June 2008
Available online 1 July 2008

Keywords:
Hypothalamus
Patch clamp
Single cell RT-PCR
Glibenclamide

ABSTRACT

Although the novel satiety factor nesfatin-1 has been shown to influence feeding behavior through effects on melanocortin signaling, the specific hypothalamic neuronal substrates through which such effects are mediated have yet to be elucidated. To identify neuronal cell types potentially important in mediating nesfatin-1's effects, whole cell current clamp recordings were made from hypothalamic arcuate nucleus neurons and the effects of bath applied nesfatin-1 on membrane excitability determined. Neurons then underwent phenotypic identification *post hoc* using single cell RT-PCR. Nesfatin-1 (10 nM) had effects on the majority of arcuate nucleus neurons tested, with most responsive cells hyperpolarizing following exposure. Furthermore, 9 of 11 identified NPY neurons hyperpolarized in response to nesfatin-1 exposure. Pharmacological experiments revealed that glibenclamide (500 nM), an ATP-sensitive potassium conductance antagonist, prevented nesfatin-1-induced hyperpolarization. Therefore, nesfatin-1-induced inhibition of feeding may be mediated through the inhibition of orexigenic NPY neurons.

1. Introduction

The arcuate nucleus of the hypothalamus is an integral component of the central control of feeding behavior. Here signals that indicate the metabolic state of the animal are received and processed following which the activity of either orexigenic NPY neurons or anorexigenic αMSH-containing neurons is increased (Abizaid et al., 2006; Schwartz et al., 2000; Zigman and Elmquist, 2003). Over the last decade several peptides have been identified as satiety signals, including one of the most recently described satiety peptides, nesfatin-1 (Oh-I et al., 2006). This peptide arises from cleavage of the calcium and DNA-binding protein nucleobindin-2 yielding an 82 amino acid product that, when injected intracerebroventricularly, reduces feeding. Moreover, inactivation of endogenous nesfatin-1 with a neutralizing antibody increases feeding, underscoring the potential importance of this peptide in the central control of appetite. Nesfatin-1 is expressed in many hypothalamic nuclei, including the arcuate where levels are affected by fasting/refeeding (Brailoiu et al., 2007). Furthermore, nucleobindin-2 recently was found to belong to the adipocyte proteome presenting the possibility that nesfatin-1 may also be a peripheral satiety signal (Adachi et al., 2007). While there is good information available on the activity and distribution of nesfatin-1 in the rat, so far there has been no receptor identified for this peptide. However, results showing that increases in intracellular calcium in cultured hypothalamic neurons are inhibited by pretreatment with pertussis toxin and by exposure to inhibitors of protein kinase A indicate the receptor is likely to belong to the family of G-protein coupled receptors (Brailoiu et al., 2007).

* *Corresponding author*. Fax: +1 613 533 6880.
E-mail address: avf@queensu.ca (A.V. Ferguson).

0006-8993/$ – see front matter © 2008 Elsevier B.V. All rights reserved.
doi:10.1016/j.brainres.2008.06.084

We previously have demonstrated that nesfatin-1 has effects on the excitability of neurons within the hypothalamic paraventricular nucleus (PVN) (Price et al., 2008b). Nesfatin-1 either excited or inhibited PVN neurons without much discrimination based on electrophysiological or molecular phenotypic criteria, thereby suggesting that nesfatin-1 broadly influences the output of the PVN. Owing to the importance of the arcuate nucleus in the regulation of feeding behavior and that the arcuate nucleus receives inputs from many brain structures, such as the PVN, nucleus of the solitary tract (NTS) and the raphe nuclei, that possess nesfatin-1 expressing neurons (Brailoiu et al., 2007; Ricardo and Koh, 1978) we now have performed electrophysiological recordings on neurons within the arcuate nucleus, examining how nesfatin-1 influences the excitability of these neurons.

2. Results

2.1. *Nesfatin-1 influences the excitability of the majority of neurons in the arcuate nucleus*

The results presented here represent data from a total of 102 arcuate neurons from which whole cell recordings were obtained to assess nesfatin-1 effects on membrane potential.

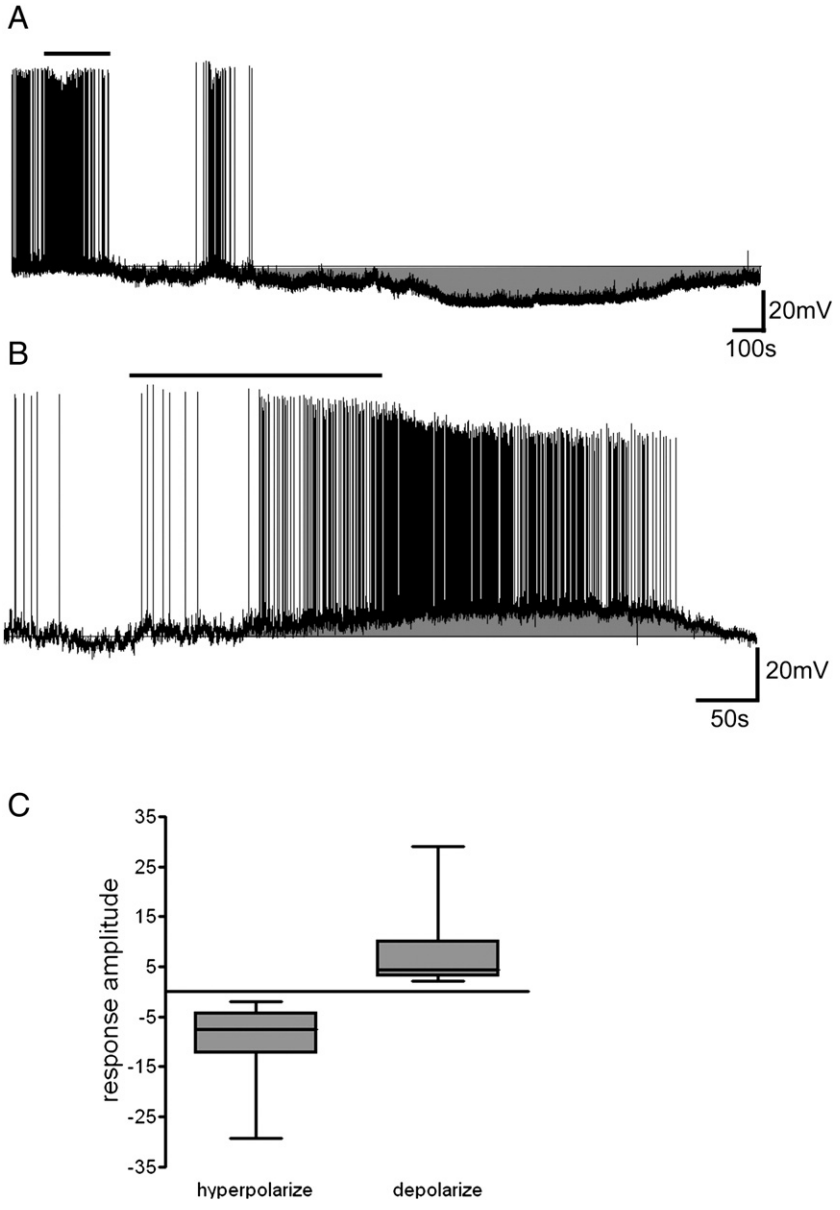

Fig. 1 – Nesfatin-1 influences the excitability of neurons in the hypothalamic arcuate nucleus. (A) Current clamp recording trace showing the reversible hyperpolarization of an arcuate nucleus neuron induced by 10 nM nesfatin-1. Bar over trace indicates duration of nesfatin-1 application. (B) In another arcuate nucleus neuron 10 nM nesfatin-1 reversibly depolarized the cell and markedly increased the frequency of action potential firing. (C) Box and whiskers plot showing the median and distribution of hyperpolaring ($n=37$) and depolarizing ($n=24$) responses induced by 10 nM nesfatin-1 in arcuate nucleus neurons.

Cytoplasm was collected from 84 of these cells at the completion of recordings to permit later phenotypic identification (see NPY neurons below). Whole cell current clamp recordings demonstrated that bath application of 10 nM nesfatin-1 caused significant changes in membrane potential in a total of 65% of arcuate neurons tested with 39.4% demonstrating a slowly developing and reversible membrane hyperpolarization (Fig. 1A). An additional subset of nesfatin-1 responsive neurons (25.5%) showed temporally similar depolarizations in response to peptide exposure as illustrated in Fig. 1B. Overall, the mean amplitude of nesfatin-1-induced hyperpolarization was −9.0±1.0 mV (n=37) and depolarization was 6.9±1.2 mV (n=24) (Fig. 1C). There was no apparent relationship between initial control membrane potential and the resulting responses, whether hyperpolarizing or depolarizing.

We next undertook experiments to examine if hyperpolarizing and depolarizing actions of nesfatin-1 were observed when applied in the presence of the voltage-gated sodium channel blocker TTX (n=9; Fig. 2A,B). These responses in TTX occurred in a similar proportion of neurons as seen in its absence (Fig. 2C; chi-squared p=0.94), indicating that the responsiveness of arcuate nucleus neurons to nesfatin-1 was not dependent on action potential mediated inputs from local interneurons, and was thus most likely the result of direct effects on the recorded neuron.

2.2. *Arcuate nucleus NPY neurons are predominantly hyperpolarized by nesfatin-1*

In the initial description of the nesfatin-1 (Oh et al., 2006) it was demonstrated that intracerebroventricular injection of this peptide resulted in an inhibition of feeding in rats and that the melanocortin system was involved in mediating this effect. Therefore, we next attempted to combine our single cell recording techniques with *post hoc* single cell RT-PCR to define the effects of nesfatin-1 on NPY and/or POMC expressing arcuate neurons. Using this technique we were able to identify 17/84 GAPDH-positive arcuate neurons which expressed mRNA for NPY in which we had tested the effects of nesfatin-1. A total of 11 of 17 NPY-expressing neurons responded to nesfatin-1, with the vast majority of these responsive NPY neurons (82%) showing hyperpolarizing responses to peptide administration (Fig. 3A,B). We only were able to obtain recordings from three POMC-positive neurons during our experiments and so we were not able to compare the effects of nesfatin-1 on these cells.

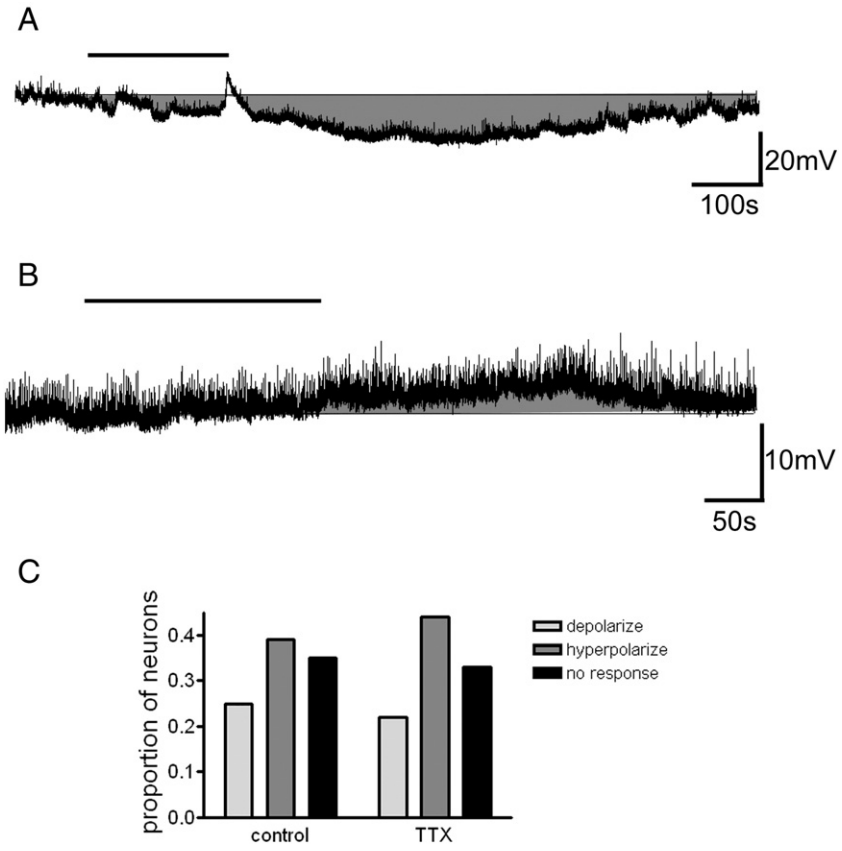

Fig. 2 – Nesfatin-1-induced effects on excitability are preserved in the presence of 1 μM TTX. (A) Current clamp recording trace recorded in the continued presence of TTX showing 10 nM nesfatin-1 induced reversible hyperpolarization of an arcuate nucleus neuron. Bar over the trace indicates the duration of nesfatin-1 application (B) In another neuron, 10 nM nesfatin-1 induced a reversible depolarization of the cell in the presence of TTX. (C) Bar graph showing the proportion of neurons that depolarized, hyperpolarized and did not respond to nesfatin-1 in the absence and presence of 1 μM TTX.

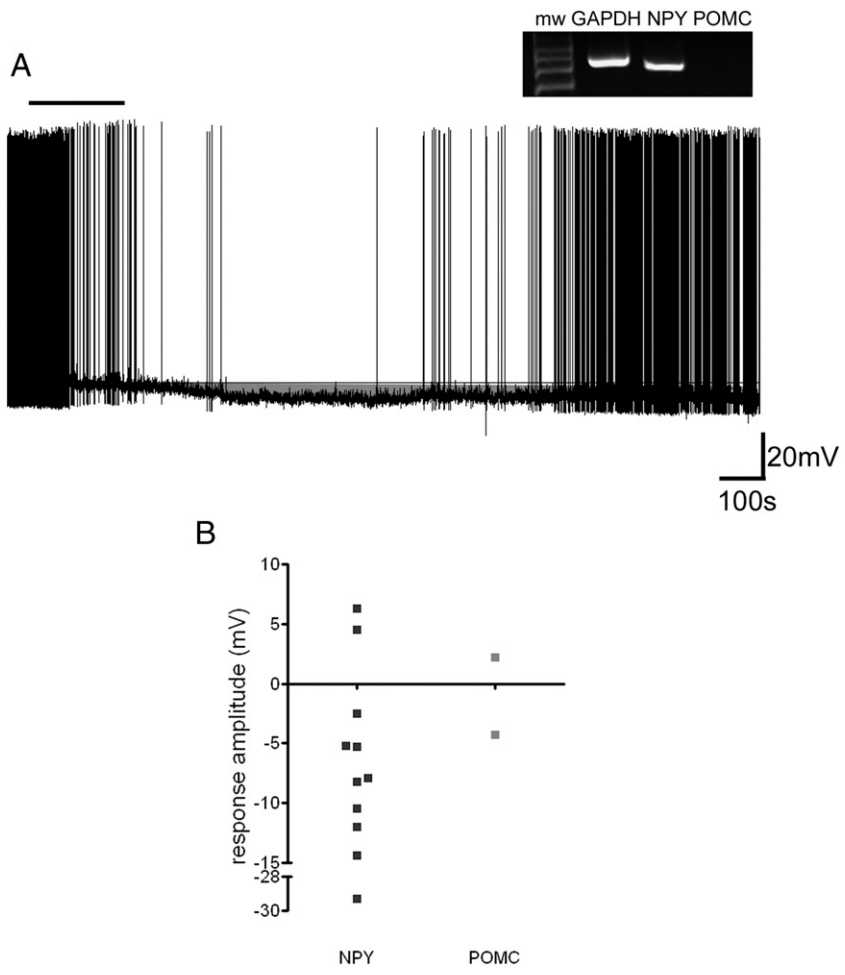

Fig. 3 – NPY neurons are predominantly hyperpolarized by nesfatin-1. (A) Current clamp recording trace showing the reversible hyperpolarization of an arcuate nucleus neuron induced by 10 nM nesfatin-1. This neuron was identified *post hoc* via single cell RT-PCR as an NPY-expressing cell (inset). Bar indicates the duration of nesfatin-1 exposure. (B) Summary graph showing the amplitude of responses induced by 10 nM nesfatin-1 for neurons that were identified by single cell RT-PCR as NPY or POMC expressing.

2.3. *Nesfatin-1-induced hyperpolarization is mediated through activation of an ATP-sensitive potassium conductance*

We next examined the conductances responsible for these effects of nesfatin-1 by applying hyperpolarizing current step pulses to neurons to assess input resistance changes induced by nesfatin-1. Voltage/current (V/I) plots generated from neurons before and following nesfatin-1-induced hyperpolarization had points of convergence indicating a potassium conductance with a reversal potential of −96 ±6.8 mV (n=6) was activated (Fig. 4A). Conversely, V/I plots for neurons that depolarized following nesfatin-1 application intersected with control plots at a membrane potential of −55±4.5 mV (n=3) suggesting the activation of a non-selective cation conductance underlies this action of nesfatin-1 (Fig. 4B).

The satiety-inducing factors insulin and leptin have electrophysiological effects in the arcuate nucleus which are in part due to the activation of an ATP-sensitive potassium conductance (K_{ATP}) (van den Top et al., 2007). To determine if this conductance was responsible for nesfatin-1-induced hyperpolarization, we used the specific antagonist glibenclamide (500 nM) to determine if hyperpolarizing responses induced by nesfatin-1 could be reversed or abolished by pharmacological blockade of this conductance. Glibenclamide by itself caused membrane depolarization in a subset of neurons tested indicating some neurons possess a basal level of K_{ATP} channel activity under our recording conditions (mean 7.2±1.0 mV; 6 out of 13 neurons). However, when nesfatin-1 was applied to neurons pretreated with glibenclamide, no membrane hyperpolarizations were observed while depolarizing responses could still be induced (Fig. 4C; n=9). Furthermore, when applied following the establishment of nesfatin-1-induced hyperpolarization and in the presence of nesfatin-1, glibenclamide caused a return to near baseline membrane potential in all but one neuron tested (Fig. 4D,E). There was no significant difference between the membrane potential recorded during the control period and that recorded following application of glibenclamide (paired t-test p=0.8357).

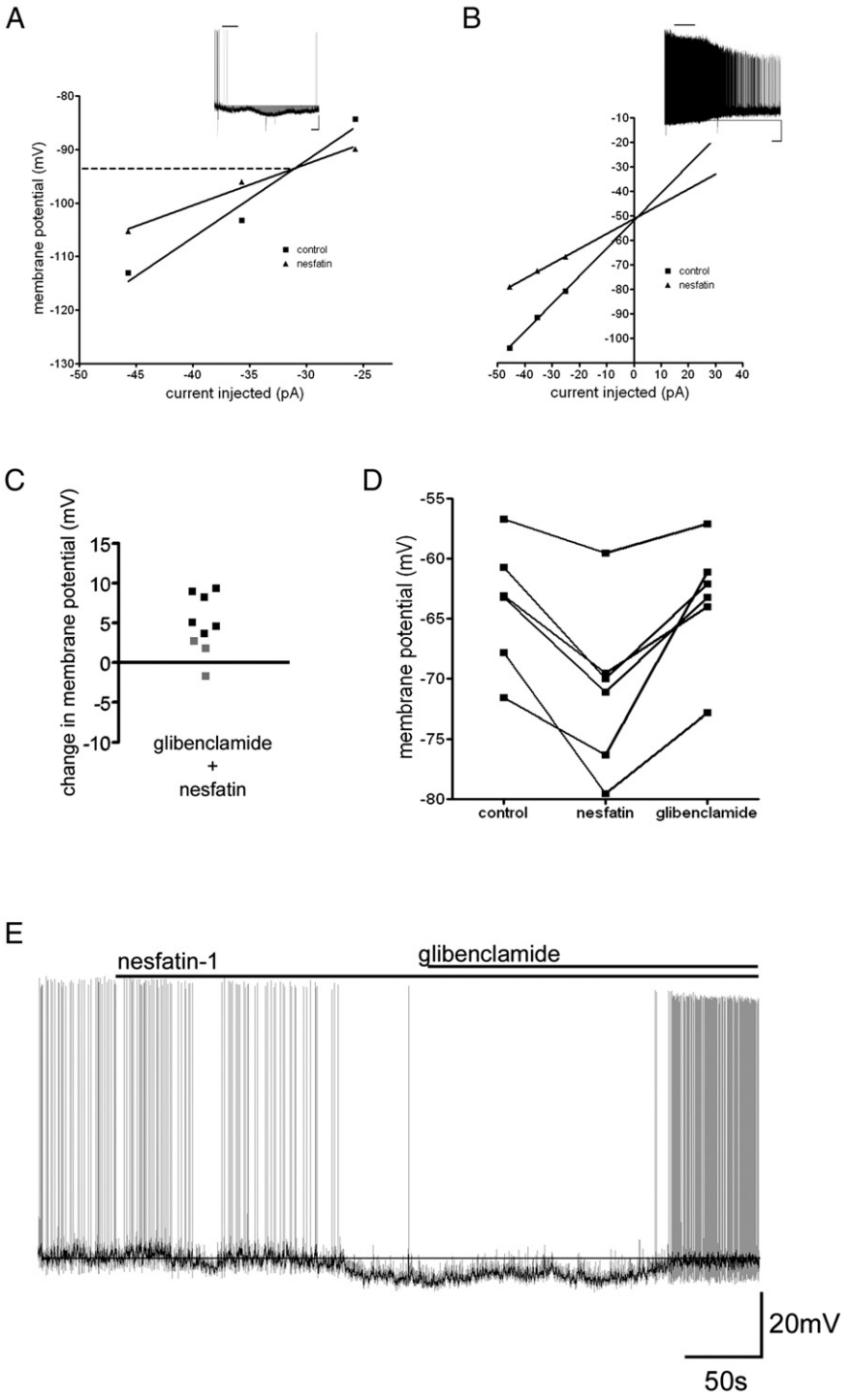

Fig. 4 – K_{ATP} conductance mediates nesfatin-1-induced hyperpolarization of arcuate nucleus neurons. (A) V/I plot showing the change in input resistance that accompanied hyperpolarization of an arcuate nucleus neuron following exposure to 10 nM nesfatin-1. The point of intersection indicates the reversal potential for the conductance activated, which is near the calculated reversal potential for potassium ions (–100 mV). Inset current clamp recording trace shows the response of the neuron to nesfatin-1 (scale 20 mV and 100 s). (B) V/I plot showing the change in input resistance that accompanied the depolarization of a different neuron following nesfatin-1 exposure. Inset current clamp recording trace shows the depolarizing response of this neuron to nesfatin-1 (scale 20 mV and 100 s). (C) Scatter plot showing the change in membrane potential following application of nesfatin-1 recorded in neurons pretreated with 500 nM glibenclamide. Black squares represent responses that surpass the two standard deviation threshold, while grey squares represent cells that did not respond to nesfatin-1 based on this criterion. (D) Graph summarizing the effect 500 nM glibenclamide has on returning membrane potential to control levels following nesfatin-1 application. (E) Current clamp recording (light trace) showing the effectiveness of the K_{ATP} antagonist glibenclamide (500 nM) to inhibit the hyperpolarization induced by nesfatin-1. Dark trace is the recording after smoothing to remove action potentials and accentuate the effects glibenclamide has on membrane potential.

3. Discussion

The regulation of feeding behavior involves the integration of peripherally and centrally derived signals to establish the energy state of the animal. Nesfatin-1 may represent one of the more important centrally derived peptidergic signals involved in this process. This peptide inhibits feeding, while antibodies against native nesfatin-1 stimulate feeding (Oh et al., 2006). Immunohistochemical studies have found this peptide to be located in neuronal cell bodies in the arcuate nucleus as well as in the brain stem and in several other hypothalamic nuclei (Brailoiu et al., 2007; Oh-I et al., 2006). Interestingly, refeeding following fasting activated and induced cFos expression in nesfatin-1-expressing neurons of the PVN. As a result afferents from the PVN may be an important nesfatin-1 source to the arcuate nucleus (Kohno et al., 2008). Similarly, the NTS receives inputs directly from the periphery and indirectly via the area postrema, a circumventricular organ that lacking a normal blood brain barrier can detect satiety-inducing factors circulating in the blood (Price et al., 2008a). Therefore, nesfatin-1 from NTS-derived afferents may also be an important source to the arcuate nucleus. It should also be mentioned that nesfatin-1 has been shown to cross the blood brain barrier and if it is indeed also found in the blood, then circulating nesfatin-1 may be detectable by the arcuate nucleus (Pan et al., 2007; Price et al., 2007).

To begin to understand the mechanisms that lead to nesfatin-1-induced inhibition of feeding we have performed *in vitro* electrophysiological experiments examining the effect of nesfatin-1 on the excitability of neurons in nuclei where this peptide is present. In an earlier study we found nesfatin-1 to have both excitatory and inhibitory actions on neurons within the PVN (Price et al., 2008b). However, the frequency of occurrence of excitation versus inhibition amongst neurons expressing mRNA for different neuropeptides or with different electrophysiological fingerprints was similar, as a result clues to understanding how nesfatin-1 mediates a reduction in feeding were not overtly apparent.

In the current study we show that in the arcuate nucleus, as seen in the PVN, both excitatory and inhibitory responses were observed. However, in the arcuate nucleus NPY-expressing neurons were predominantly inhibited by nesfatin-1. NPY neurons together with POMC neurons are the major substrate in the arcuate nucleus through which factors that indicate the energy and feeding state of the animal act (Parton et al., 2007; Schwartz et al., 2000; Zigman and Elmquist, 2003). Importantly, NPY neurons exert an inhibitory influence on the POMC neurons further promoting feeding (Cone, 2005; Cowley et al., 2001; Roseberry et al., 2004). Nesfatin-1-mediated inhibition of NPY neurons is therefore consistent with the original description of nesfatin-1-induced inhibition of feeding which was found to be sensitive to an antagonist of melanocortin receptors (Oh-I et al., 2006). In this study POMC neurons were rarely encountered. While some neurons with this phenotype did indeed respond to nesfatin-1, it is not reasonable to draw any further conclusions. Further studies employing GFP-POMC mice, which were developed to address the difficulty in locating POMC neurons in arcuate nucleus slices (Cowley et al., 2001), would facilitate exploring further the effects of nesfatin-1 on POMC neurons.

The majority of NPY-expressing neurons occurring along the ventricular surface in the arcuate nucleus are known to express mRNA for $Kir_{6.2}$ channel (Dunn-Meynell et al., 1998). In this study we found that the hyperpolarization induced by nesfatin-1 was not observed when the K_{ATP} channel antagonist glibenclamide was present in the bathing solution at submicromolar concentrations. Further, glibenclamide also caused nesfatin-induced hyperpolarizations to return to baseline. Taken together these observations support the hypothesis that K_{ATP} channels mediate nesfatin-1-induced hyperpolarization, taking into consideration that some of the effects of glibenclamide in the latter experiment might be due to its ability to depolarize arcuate neurons in the absence of nesfatin-1. Two other important satiety factors, leptin and insulin, utilize these channels to mediate their actions in the arcuate nucleus indicating that the activation of K_{ATP} channels may be a common route through which signals that inhibit feeding via the arcuate nucleus exert their influence (Spanswick et al., 1997, 2000).

In summary, our electrophysiological and molecular studies of neurons responsive to the novel peptide nesfatin-1 in the arcuate nucleus indicate that this peptide may exert its anorexigenic effects on feeding behavior by inhibiting arcuate NPY neurons, likely via activation of K_{ATP} channels.

4. Experimental procedures

4.1. *Slice preparation*

All animal procedures conformed to the standards of the Canadian Council on Animal Care and were approved by the Queen's University Animal Care Committee. Male Sprague Dawley rats (Charles River, Quebec, Canada) aged postnatal day 21 to 27 (approximately 50–100 g) were used in the preparation of hypothalamic slices. Rats were quickly decapitated and the brain dissected out and placed into ice cold carbogenated slicing solution, consisting of (in mM): 87 NaCl, 2.5 KCl, 25 $NaHCO_3$, 0.5 $CaCl_2$, 7 $MgCl_2$, 1.25 NaH_2PO_4, 25 glucose and 75 sucrose. A tissue block containing the hypothalamus was obtained and 300 μm coronal slices cut using a vibratome. Slices were then stored in a water bath at 32 °C for at least 1 h, before recordings commenced, in carbogenated artificial cerebrospinal fluid (ACSF) composed of (in mM): 126 NaCl, 2.5 KCl, 26 $NaHCO_3$, 2 $CaCl_2$, 2 $MgCl_2$ 1.25 NaH_2PO_4 and 10 glucose.

4.2. *Electrophysiology*

Slices containing the arcuate nucleus were placed in a chamber that was continuously perfused at approximately 2 ml/min with carbogenated ACSF heated to between 28° and 32 °C. Neurons were visualized using an infra-red differential interference contrast system on an upright microscope (Nikon, Japan). Whole cell current and voltage clamp recordings were made using a Multiclamp 700B amplifier (Molecular Devices, Sunnyvale CA) and sampled using a Micro1401 interface and Spike2 software (Cambridge Electronic Design,

Cambridge UK) for offline analysis. Digitization rate was 5 kHz and signals were filtered at 10 kHz. Electrodes were filled with an intracellular solution that was prepared under RNase-free conditions and contained (in mM): 125 potassium gluconate, 2 $MgCl_2$, 5.5 EGTA, 10 KCl, 0.1 $CaCl_2$, 2 NaATP and 10 Hepes (pH 7.2–7.3 with KOH). When filled with this solution electrodes had resistances of 3 to 7 MΩ. Neurons that did not have overshooting action potentials with amplitudes over 60 mV or did not possess a stable baseline were excluded from further experiments. Nesfatin-1 was applied to the cell via the bath perfusion. Neurons were said to have responded to nesfatin-1 if there was a change in membrane potential that was at least twice the amplitude of the standard deviation of the mean baseline membrane potential. This value was obtained by taking an average and standard deviation of all the points during the 50 s control period immediately prior to peptide application. For neurons with on going spiking activity, the voltage trace was smoothed (time constant 0.2 s) so that the presence of action potentials did not inflate the size of the standard deviation and create false negatives. Smoothing had no effect on the mean baseline or response amplitude. Response amplitudes were quantified by subtracting the mean baseline membrane potential from the peak membrane potential, averaged over a 50 s segment of the recording showing the maximal effect.

4.3. *Single cell RT-PCR*

Following the completion of each single cell recording, gentle suction was applied to the electrode interior and, under visual control, the cytoplasmic contents were collected. The electrode was then carefully withdrawn from the cell until the electrode detached, forming an outside-out patch. The electrode tip was subsequently broken and its contents aspirated into a 0.5 ml microcentrifuge tube. Prior to the reverse transcriptase reaction cytoplasm was treated for 30 min at 37 °C with DNase (Fermentas, Burlington, Ont., Canada). Immediately following inactivation of the DNase the reverse transcriptase reaction was initiated via adding to the cytoplasm (approximate final concentration): dithiothreitol (26 mM), dNTPs (3 mM), random hexamer primers (3 μM), $MgCl_2$ (4 mM), RNase inhibitor (20 U) and superscript II reverse transcriptase (100 U) (all from Invitrogen, Burlington, Ontario, Canada). The reverse transcriptase reaction ran overnight at 37 °C after which the cDNA was stored at −80 °C until the start of the multiplex reaction. A multiplex PCR approach was employed to amplify the cDNA obtained from the reverse transcriptase reaction using primers specific for glyceraldehyde 3-phosphate dehydrogenase (GAPDH: Outside Sense 5′: GAT GGT GAA GGT CGG TGT G Antisense 5′: GGG CTA AGC AGT TGG TGG T Inside Sense 5′: TAC CAG GGC TGC CTT CTC T Antisense 5′: CTC GTG GTT CAC ACC CAT C); neuropeptide Y (NPY: Outside Sense 5′: GCC CAG AGC AGA GCA CCC Antisense 5′: CAA GTT TCA TTT CCC ATC ACC A Inside Sense 5′: CAG AGA CCA CAG CCC GCC Antisense 5′: TCT TCA AGC CTT GTT CTG GGG); and pro-opiomelanocortin (POMC: Outside Sense 5′: CGA GAT TCT GCT ACA GTC GCT CA Antisense 5′: TCT CGG CGA CAT TGG GGT ACA Inside Sense 5′: CCC TGT TGC TGG CCC TCC TG 5′: CTC CCC CCG CCG TCT CTT CC). The first step was a multiplex reaction containing primers (outside) for all the genes of interest along with cDNA from the single cell. The second reaction was a nested PCR reaction using a single set of primers (inside) for each gene of interest. The initial multiplex reaction was performed in a 100 μl volume using the reagents provided with the Qiagen Multiplex kit (Qiagen, Mississauga, Ontario, Canada) and 0.2 μM of each primer. Each reaction was denatured at 70 °C, followed by a final extension step for 10 min at 72 °C temperature protocol consisting of 30 s at 94 °C, 90 s at 60 °C and 90 s at 72 °C. The final product in early experiments was diluted 1:1000 and used as the template for the next round of PCR. In later experiments the first round product was used undiluted as template for the second round of PCR. The second round of PCR consisted of individual 50 μl reactions for each of the genes of interest. Reactions were done again using the reagents contained in the Qiagen Multiplex kit and 0.2 μM of each primer. The reaction mixture was cycled 30 times through the same temperature protocol as indicated above, afterwards the PCR products were run on a 2% (w/v) agarose gel containing ethidium bromide. Sequencing of PCR products was periodically performed to confirm identities (Robarts Institute, London, Ontario, Canada).

4.4. *Chemicals and drugs*

Salts used in the preparation of the intracellular solution and normal and high sucrose ACSF were obtained from Sigma (Oakville, Ontario, Canada). Nesfatin-1 was obtained was obtained from Phoenix Pharmaceuticals (Burlingame, CA), Tetrodotoxin (TTX) citrate was obtained from Alomone Laboratories (Jerusalem, Israel) and glibenclamide was obtained from Tocris Bioscience (Ellisville, Mo).

Acknowledgments

We would like to thank Ms. Christie Hopf for technical assistance. This work was supported by funding from the NIH (grant HL66023 to W.K.S. and A.V.F.).

REFERENCES

Abizaid, A., Gao, Q., Horvath, T.L., 2006. Thoughts for food: brain mechanisms and peripheral energy balance. Neuron 51, 691–702.

Adachi, J., Kumar, C., Zhang, Y., Mann, M., 2007. In-depth analysis of the adipocyte proteome by mass spectrometry and bioinformatics. Mol. Cell Proteomics 6, 1257–1273.

Brailoiu, G.C., Dun, S.L., Brailoiu, E., Inan, S., Yang, J., Chang, J.K., Dun, N.J., 2007. Nesfatin-1: distribution and interaction with a G protein-coupled receptor in the rat brain. Endocrinology 148, 5088–5094 Oct 2007.

Cone, R.D., 2005. Anatomy and regulation of the central melanocortin system. Nat. Neurosci. 8, 571–578.

Cowley, M.A., Smart, J.L., Rubinstein, M., Cerdan, M.G., Diano, S., Horvath, T.L., Cone, R.D., Low, M.J., 2001. Leptin activates anorexigenic POMC neurons through a neural network in the arcuate nucleus. Nature 411, 480–484.

Dunn-Meynell, A.A., Rawson, N.E., Levin, B.E., 1998. Distribution and phenotype of neurons containing the ATP-sensitive K+ channel in rat brain. Brain Res. 814, 41–54.

Kohno, D., Nakata, M., Maejima, Y., Shimizu, H., Sedbazar, U., Yoshida, N., Dezaki, K., Onaka, T., Mori, M., Yada, T., 2008.

Nesfatin-1 neurons in paraventricular and supraoptic nuclei of the rat hypothalamus coexpress oxytocin and vasopressin and are activated by refeeding. Endocrinology 149, 1295–1301.
Oh-I., Shimizu, H., Satoh, T., Okada, S., Adachi, S., Inoue, K., Eguchi, H., Yamamoto, M., Imaki, T., Hashimoto, K., Tsuchiya, T., Monden, T., Horiguchi, K., Yamada, M., Mori, M., 2006. Identification of nesfatin-1 as a satiety molecule in the hypothalamus. Nature 443, 709–712.
Pan, W., Hsuchou, H., Kastin, A.J., 2007. Nesfatin-1 crosses the blood–brain barrier without saturation. Peptides 28, 2223–2228.
Parton, L.E., Ye, C.P., Coppari, R., Enriori, P.J., Choi, B., Zhang, C.Y., Xu, C., Vianna, C.R., Balthasar, N., Lee, C.E., Elmquist, J.K., Cowley, M.A., Lowell, B.B., 2007. Glucose sensing by POMC neurons regulates glucose homeostasis and is impaired in obesity. Nature 449, 228–232.
Price, C.J., Hoyda, T.D., Ferguson, A.V., 2008a. The area postrema: a brain monitor and integrator of systemic autonomic state. Neuroscientist 14, 182–194.
Price, C.J., Hoyda, T.D., Samson, W.K., Ferguson, A.V., 2008b. Nesfatin-1 influences the excitability of paraventricular nucleus neurones. J. Neuroendocrinol. 20, 245–250.
Price, T.O., Samson, W.K., Niehoff, M.L., Banks, W.A., 2007. Permeability of the blood–brain barrier to a novel satiety molecule nesfatin-1. Peptides 28, 2372–2381.
Ricardo, J.A., Koh, E.T., 1978. Anatomical evidence of direct projections from the nucleus of the solitary tract to the hypothalamus, amygdala, and other forebrain structures in the rat. Brain Res. 153, 1–26.
Roseberry, A.G., Liu, H., Jackson, A.C., Cai, X., Friedman, J.M., 2004. Neuropeptide Y-mediated inhibition of proopiomelanocortin neurons in the arcuate nucleus shows enhanced desensitization in ob/ob mice. Neuron 41, 711–722.
Schwartz, M.W., Woods, S.C., Porte Jr., D., Seeley, R.J., Baskin, D.G., 2000. Central nervous system control of food intake. Nature 404, 661–671.
Spanswick, D., Smith, M.A., Groppi, V.E., Logan, S.D., Ashford, M.L., 1997. Leptin inhibits hypothalamic neurons by activation of ATP-sensitive potassium channels. Nature 390, 521–525.
Spanswick, D., Smith, M.A., Mirshamsi, S., Routh, V.H., Ashford, M.L., 2000. Insulin activates ATP-sensitive K+ channels in hypothalamic neurons of lean, but not obese rats. Nat. Neurosci. 3, 757–758.
van den Top, M., Lyons, D.J., Lee, K., Coderre, E., Renaud, L.P., Spanswick, D., 2007. Pharmacological and molecular characterization of ATP-sensitive K(+) conductances in CART and NPY/AgRP expressing neurons of the hypothalamic arcuate nucleus. Neuroscience 144, 815–824.
Zigman, J.M., Elmquist, J.K., 2003. Minireview: From anorexia to obesity—the yin and yang of body weight control. Endocrinology 144, 3749–3756.